REPORT DOCUMENTATION PAGE

Form Approved
OMB No. 0704-0188

1. REPORT DATE *(DD-MM-YYYY)*	2. REPORT TYPE	3. DATES COVERED *(From - To)*
24-05-2011	Journal Article	

4. TITLE AND SUBTITLE

Modeling the Combustion of a Sub-micron Aluminum Particle

5a. CONTRACT NUMBER

5b. GRANT NUMBER

5c. PROGRAM ELEMENT NUMBER

6. AUTHOR(S)
John Buckmaster, Thomas L. Jackson, and Nick Glumac

5d. PROJECT NUMBER

5f. WORK UNIT NUMBER
300510TM

7. PERFORMING ORGANIZATION NAME(S) AND ADDRESS(ES)

Air Force Research Laboratory (AFMC)
AFRL/RZSA
10 E. Saturn Blvd.
Edwards AFB CA 93524-7680

8. PERFORMING ORGANIZATION REPORT NUMBER

AFRL-RZ-ED-JA-2011-178

9. SPONSORING / MONITORING AGENCY NAME(S) AND ADDRESS(ES)

Air Force Research Laboratory (AFMC)
AFRL/RZS
5 Pollux Drive
Edwards AFB CA 93524-7048

10. SPONSOR/MONITOR'S ACRONYM(S)

11. SPONSOR/MONITOR'S NUMBER(S)
AFRL-RZ-ED-JA-2011-178

12. DISTRIBUTION / AVAILABILITY STATEMENT

Approved for public release; distribution unlimited (PA #11220).

13. SUPPLEMENTARY NOTES
For publication in Combustion and Flame.

14. ABSTRACT

We examine the shrinking-core model of aluminum combustion, one that has been proposed for sub-micron drop diameters. In this model a core of liquid aluminum is surrounded by alumina through which O atoms diffuse to the aluminum surface. It is shown that the volume changes intrinsic to this model necessarily lead to fracturing of the alumina and the creation of cracks and voids. A simple mathematical model is described which, because of the length and time scales, is quasi-steady, permitting analytical solutions. When the drop is sufficiently small this leads to a simple formula for the burn time as a function of the atmospheric pressure, temperature, and oxygen concentration, which is tested against experimental data. By introducing a fractal ingredient into the description, motivated by the fracturing, it is possible to generate agreement with experimental data on the variations of burn time with drop diameter, a $d^{0.25}$-t law in contrast with the familiar d^2-t law of classical fuel-drop combustion. For larger drop diameters a non-linear differential equation for the burn rate is derived whose integration yields the burn time as a function of drop diameter and shows a transition from the $d^{0.25}$ law to a d^2 law.

15. SUBJECT TERMS

16. SECURITY CLASSIFICATION OF:			17. LIMITATION OF ABSTRACT	18. NUMBER OF PAGES	19a. NAME OF RESPONSIBLE PERSON
					Mr. S. Alex Schumaker
a. REPORT	b. ABSTRACT	c. THIS PAGE	SAR	14	19b. TELEPHONE NUMBER *(include area code)*
Unclassified	**Unclassified**	**Unclassified**			N/A

Modeling the combustion of a sub-micron aluminum particle

John Buckmaster*, Thomas L Jackson†, and Nick Glumac‡

May 18, 2011

Abstract

We examine the shrinking-core model of aluminum combustion, one that has been proposed for sub-micron drop diameters. In this model a core of liquid aluminum is surrounded by alumina through which O atoms diffuse to the aluminum surface. It is shown that the volume changes intrinsic to this model necessarily lead to fracturing of the alumina and the creation of cracks and voids. A simple mathematical model is described which, because of the length and time scales, is quasi-steady, permitting analytical solutions. When the drop is sufficiently small this leads to a simple formula for the burn time as a function of the atmospheric pressure, temperature, and oxygen concentration, which is tested against experimental data. By introducing a fractal ingredient into the description, motivated by the fracturing, it is possible to generate agreement with experimental data on the variations of burn time with drop diameter, a $d^{0.25}$-t law in contrast with the familiar d^2-t law of classical fuel-drop combustion. For larger drop diameters a non-linear differential equation for the burn rate is derived whose integration yields the burn time as a function of drop diameter and shows a transition from the $d^{0.25}$ law to a d^2 law.

keywords: nano-aluminum, shrinking-core, fracture, fractal, combustion, burn-time/diameter laws

1 Introduction

The combustion of aluminum particles is an important subject, if only because such particles are a common ingredient of heterogeneous rocket propellants. A large literature exists for particles of diameter greater than 100 μm or so (see the review of Beckstead [1]), and the basic structure of the combustion field is that of the classical fuel drop. It is well known that the so-called d^2 law is then relevant, a linear relation between the square of the diameter and the burn time. This follows directly from a simple dimensional argument, one that we shall repeat here as pedagogical texts frequently muddy the issue.

Almost all diffusion flames are characterized by a large Damköhler number, so that the chemistry is fast, and does not define a relevant time scale. Accordingly, there are only two relevant lengths: the drop diameter d; and the diffusion length $\rho D/M$ where M is the mass flux per unit area, proportional to $(\mathrm{d}/\mathrm{d}t)d$. It follows that $d \propto 1/M$, whence $(\mathrm{d}/\mathrm{d}t)d^2 = \text{const}$.

More recent research efforts have been concerned with sub-micron particles, even particles on the nano scale, and important experimental work has been carried out. One immediate

*Buckmaster Research, Urbana, IL 61801.

†Computational Science and Engineering, University of Illinois at Urbana-Champaign, Urbana, IL 61801. Also, IllinoisRocstar LLC, Urbana, IL, 61826.

‡Mechanical Science and Engineering, University of Illinois at Urbana-Champaign, Urbana, IL 61801.

observation is that a reduction in size decreases the diffusion time scale and so for sufficiently small particles the fast-chemistry assumption will be false, and the d^2 law will no longer prevail. This has been confirmed experimentally. Modeling efforts have been reported by Zachariah [2, 3],who considers what is called the shrinking-core model.

The shrinking-core model is spherically symmetric. At the core is a sphere of liquid aluminum (aluminum is liquid between 933 K and 3100 K), and surrounding this sphere is a shell of solid alumina (Al_2O_3, melting point 2345 K). When immersed in a hot atmosphere containing oxygen, some of the latter dissociates heterogeneously at the oxide surface and oxygen atoms diffuse through the shell to react at the aluminum surface. This surface retreats with time and the traveling reaction front is a transition zone between the aluminum and the alumina. The diffusive flux of oxygen to the front is comparable to the mass flux through it as, overall, it sustains the reaction

$$2Al + 3O \rightarrow Al_2O_3 \tag{1}$$

one in which 53.96 mass units of aluminum are consumed for 48 mass units of oxygen.

2 Some Geometry Issues

Here we discuss some geometrical issues that arise because of the material conversion in the drop/particle. These arise by consideration of the mass of aluminum and oxygen that goes into the formation of the alumina. As supplied, aluminum particles have a thin coating of alumina (2-4 nm thick) and we neglect this in our discussion.

Consider a sphere (aluminum) of initial diameter d_i which is converted to a sphere of alumina of diameter d_f. Then the initial drop mass is

$$\frac{\pi}{6} d_i^3 \rho_{al},$$

the final mass is

$$\frac{\pi}{6} d_f^3 \rho_{ala},$$

and the added mass of oxygen is

$$\frac{48}{53.96} \frac{\pi}{6} d_i^3 \rho_{al}.$$

Mass conservation then requires ($\rho_{al} = 2700$ kg/m^3, $\rho_{ala} = 3950$ kg/m^3)

$$\frac{d_f}{d_i} = (1.2916)^{\frac{1}{3}} = 1.0890.$$

Thus one might expect an 8.9% increase in diameter.

However, let us examine the neighborhood of the front, which we suppose is located at a radius s at time t. This front separates aluminum from previously generated alumina, and is moving with speed u into the aluminum. At the same time the boundary between previously generated alumina and newly generated alumina is moving with speed v in the opposite direction; this speed arises because of the volume demands of the alumina. Then in an infinitesimal time Δt, and considering unit area of front, the mass of aluminum consumed is

$$\rho_{al} u \Delta t,$$

the mass of alumina produced is

$$\rho_{ala}(u+v)\Delta t,$$

and the mass of consumed oxygen is

$$\frac{48}{53.96}\rho_{ala}u\Delta t.$$

Thus

$$\frac{v}{u} = 0.2916.$$

In other words, the local (linear) argument shows that the overall particle/drop diameter increases by a factor 1.2916 over the complete burn, a 29.16% increase rather than an 8.9% increase.

To reconcile these facts we note that although alumina is a valuable ceramic with many desirable properties, it is brittle and weak in shear and tension. And so, although some deformation can be sustained, significant fracturing will occur, creating voids. If we assume that all of the adjustment is made in this way, we can calculate the effective final density of the alumina sphere by assigning its final radius, viz.

$$\frac{d_f^3}{d_i^3} = \frac{2700}{\rho_{\text{eff}}}\left[1 + \frac{48}{53.96}\right] = 1.2916^3$$

whence

$$\rho_{\text{eff}} = 2368.$$

The history of the density change can be described by considering a partial burn. Consider a point at a radius r ($\leq d/2$) fixed in the laboratory frame. As the front passes through this point it processes a shell of aluminum to create a shell of alumina of thickness δ located between r and $r+\delta$. At some later time when the front is at a radius s this shell has been displaced outwards by a distance $0.2916(r-s)$ so that it is located between $r+0.2916(r-s)$ and $r+0.2916(r-s)+\delta$. Its initial volume is $4\pi r^2\delta$ and its final volume is

$$4\pi[r + 0.2916(r-s)]^2\delta,$$

so that the final density is

$$3950[1 + 0.2916(1-s/r)]^{-2}.$$

Figure 1 is a plot of the density ratio $\rho_{\text{ratio}} = \rho/3950$ vs. $2r/d$ for different values of $2s/d$. Consider, for example, $2s/d = 1/4$. At $2r/d = 1/4$ the density ratio is equal to 1, and as r increases it falls monotonically to the value 0.6733 at $2r/d = 1$, the drop/particle boundary. The physical location of this boundary is greater than $d/2$ of course, because of the expansion. If r' is the radial measure once expansion is started a point at $r < s$ is mapped onto $r' = r$; but a point at $r > s$ is mapped onto $r' = r + 0.29(r-s)$.

One might reasonably ask whether a ceramic of which only 60% is solid and in which the void space is created by cracking and displacement can have any structural integrity, would not, in fact, disperse in fragments. Yet the latter does not occur, [4]. One possibility is that the liquid aluminum is drawn into the cracks by capillary action, a process of system self-healing, although, conceivably, outer layers could be shed. If aluminum is drawn up into a crack, gases must be pulled down through another crack to replace the volume. And when the burn is complete the alumina will have a hollow core. Hollow post-burn cores have been reported by Zachariah [3].

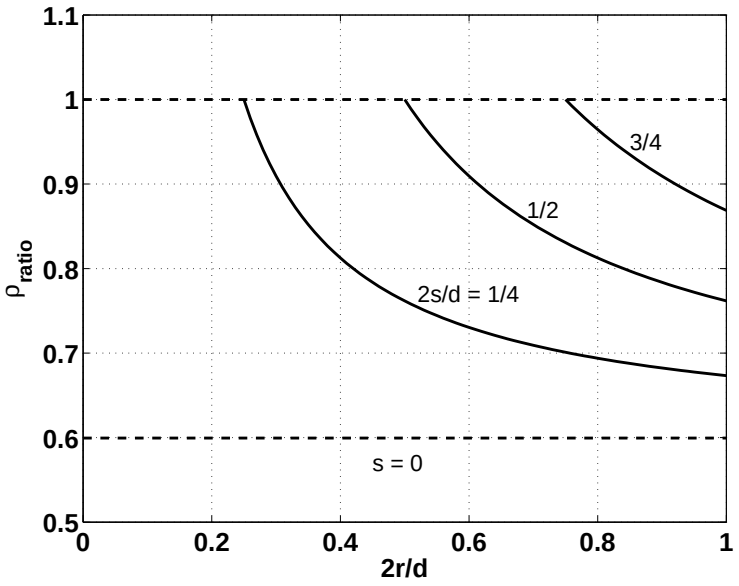

Figure 1: Density ratio ρ_{ratio} vs $2r/d$ for different $2s/d$.

3 Mathematical Model

In this section we describe the mathematical model and, from scaling considerations, describe rational approximations to the equations. A key observation is that the temperature field and the oxygen concentration field are quasi-steady so that the problem reduces to a non-linear differential equation for the location of the reacting front as a function of time. If we take some liberty with the diffusion coefficient this equation reduces to a simple expression for the front speed in terms of the atmospheric conditions (temperature, pressure, oxygen concentration). Certain free parameters (e.g. the power-law dependence on the oxygen concentration) can be chosen to fit experimental data, and for a fixed particle size ($d = 80$ nm) variations of burn time with the oxygen concentration, and burn times with temperature at two different pressures are accurately calculated. However, the predicted burn law is a linear one, and recently, Glumac [5] measured the burn times for particles of size 18, 50, 80, and 110 nm, with atmospheric conditions fixed, data which can be well fitted with a $d^{0.25}$ law. And so we have created an epistemological model by a simple modification of the derived model which forces the $d^{0.25}$ law. This modification is partly motivated by the geometric discussion of Section 2, and introduces no new parameters (apart from the 0.25). Predicted burn times differ by negligible amounts from a MatLab-generated fit to the experimental data.

Later we examine the solution sans liberties with the diffusion coefficient.

3.1 Governing Equations

We put aside the geometrical issues of Section 2 (specifically, the motion of the oxide) and write down simple field equations for the temperature and the concentration of oxygen. There is no significant convective transport in the laboratory frame, and so in both the aluminum and alumina heat conduction is governed by

$$\rho C \frac{\partial T}{\partial t} = \frac{1}{r^2}\frac{\partial}{\partial r}\left(\lambda r^2 \frac{\partial T}{\partial r}\right). \tag{2}$$

Here, T is the temperature, r the radial coordinate, t time. The density ρ, the thermal conductivity λ, and the specific heat C are assigned values appropriate to the medium. Also, in the alumina the concentration of oxygen (kg-mol/m^3) is controlled by

$$\frac{\partial c}{\partial t} = \frac{1}{r^2}\frac{\partial}{\partial r}\left(D r^2 \frac{\partial c}{\partial r}\right). \tag{3}$$

where D is the diffusion coefficient.

At the front, the temperature is continuous

$$[T]^+_- = 0, \tag{4}$$

where $(+)$ refers to the alumina side of the front.

Energy conservation is given by

$$-\left[\lambda \frac{\partial T}{\partial r}\right]^+_- = Q_s M, \tag{5}$$

if the difference in the specific heats is neglected; M is the outward mass flux through the front, and Q_s is the heat released. And the diffusive flux of oxygen to the front is related to M by

$$W_o D \left.\frac{\partial c}{\partial r}\right|^+ = \frac{3W_{ala}}{W_{al}} M, \tag{6}$$

a consequence of the stoichiometry defined by equation (1).

If the front is located at

$$r = s(t) \qquad (ds/dt < 0) \tag{7}$$

the mass flux is defined by

$$M = -\rho_{al}\frac{ds}{dt}. \tag{8}$$

The front moves because of consumption by reaction of aluminum at the surface of the aluminum drop, and we suppose that this can be described by the law

$$\frac{ds}{dt} = -K\left(\frac{c}{c_{ref}}\right)^m \left(\frac{p}{p_{ref}}\right)^q \left(\frac{T}{T_{ref}}\right)^n \exp(-E/RT + E/RT_{ref}), \tag{9}$$

where p is the pressure and the subscript $_{ref}$ denotes reference quantities to be specified.

Finally we impose boundary conditions at the outer boundary $r = d/2$ of the alumina

$$\begin{aligned} c &= c_o, \\ -\lambda\frac{dT}{dr} &= \epsilon\sigma(T^4 - T_\infty^4) + \frac{\lambda_{ala}\mathrm{Nu}}{d}(T - T_\infty), \end{aligned} \tag{10}$$

where σ is the Stefan-Boltzmann constant, ϵ is the emissivity of the alumina, and Nu is the convective Nusselt number.

Parameter	Value
ρ_{al}	2700 kg/m^3
ρ_{ala}	3950 kg/m^3
C	900 J/kg-K
D	10^{-7} m^2/s
Nu	2
Q_s	3.11×10^5 kJ/kg
ϵ	0.41
λ_{al}	250 W/m-K
λ_{ala}	25 W/m-K
σ	5.67×10^{-8} W/m^2-K^4

Table 1: Table of parameter values.

3.2 Scaling

Here we examine the equations and come to conclusions as to which terms are important and which terms are not. To this end we scale using: length $d/2$; time τ = burn time; speed $d/2\tau$. Then the non-dimensional temperature equation can be written

$$\frac{\partial T}{\partial t} = \alpha \frac{1}{r^2}\frac{\partial}{\partial r}\left(r^2 \frac{\partial T}{\partial r}\right), \qquad \alpha = \frac{4\tau\lambda}{\rho C d^2}. \tag{11}$$

In the alumina, with τ= 100μs, d=80 nm, and other data from Table 1, we find that α is roughly 10^6 and so the temperature field is strongly quasi-steady, apart from any (rapid) initial transients. Similar conclusions are true for the temperature in the aluminum (the equivalent α is 10^7) and for the oxygen concentration in the alumina (the equivalent α is 6×10^3). Since the r-dependent solution of the steady equations is singular at the origin, it follows immediately that the temperature in the aluminum does not depend on r. Moreover, the scalings reveal that the temperature gradient on the oxidizer side of the front is essentially zero, as is the gradient at $d/2$, and so the temperature in the oxidizer is likewise independent of r. The situation is not so simple for the front condition (6) involving the concentration c, for there we find a rough balance between the first order estimates of the oxygen flux and the aluminum flux.

4 Solution

As noted in Section 3.2 we may not assume that c is constant, although its description is quasi-steady. Thus

$$\frac{c}{c_{ref}} = \frac{c_o}{c_{ref}} + \frac{B}{d}\left(\frac{1}{r} - \frac{2}{d}\right) \tag{12}$$

for some B, where c_o is the value of c at the boundary, $r = d/2$. At s, $dc/dr \propto B \propto ds/dt$ so that

$$B = \frac{3W_{ala}\rho_{al}}{4W_{al}W_o D c_{ref}} s^2 \frac{ds}{dt}. \tag{13}$$

Thus c at $r = s$ is determined as a functional of s and the regression law can be written

$$\frac{ds}{dt} = -K\left(\frac{p}{p_{ref}}\right)^q \left(\frac{T}{T_{ref}}\right)^n \exp\left[-\frac{E}{RT} + \frac{E}{RT_{ref}}\right] \left[\frac{c_o}{c_{ref}} + \left(\frac{s}{d} - \frac{2s^2}{d^2}\right) \frac{3W_{ala}\rho_{al}d^2}{4W_{al}W_o D c_{ref}} \frac{d}{dt}\left(\frac{s}{d}\right)\right]^m \tag{14}$$

We do not have a great deal of confidence when assigning a value to D. Measurements indicate extraordinarily large variations with particle size and temperature, variations that are not understood. And there is no consensus on what the value of D should be, for example, for an 80 nm particle at 1500 K. The difficulty is that D can not be measured directly, but only by inference, and it is not clear what other ingredients might affect the measurements. And so it would be unwise to confine our discussion of equation (14) to the specific value of D defined in Table 1, a value proposed in [6]. We note that if D is large (10^{-5} - 10^{-6} say) the quantity in brackets can be approximated by c_o/c_{ref} and we have

$$\frac{ds}{dt} = -K\left(\frac{c_o}{c_{ref}}\right)^m \left(\frac{p}{p_{ref}}\right)^q \left(\frac{T}{T_{ref}}\right)^n \exp\left[-\frac{E}{RT} + \frac{E}{RT_{ref}}\right]. \tag{15}$$

It is worth noting that if transport of oxygen to the front is facilitated by the presence of cracks (cf Section 2), a large effective D could well be appropriate.

4.1 The large D approximation

Here we examine equation (15), and two things need attention: the value to be assigned to c_o; and the mismatch between the linear $d-t$ relation (d^1 law) predicted by (15) and recent measurements by Glumac [5] that support a $d^{0.25}$ law for particles between 18 and 110 nm in diameter.

Consider c_o first. The molar concentration of O_2 in the atmosphere is

$$n/V = xp/RT, \tag{16}$$

where n is the number of moles in the volume V, p is the pressure, xp is the partial pressure of oxygen, R the gas constant, and T the temperature. Thus with p measured in atmospheres, T in degrees Kelvin

$$n/V = 12.18\ (xp/T)\ \text{kg-mol/m}^3. \tag{17}$$

Thus for a pressure of 8 atm, a mole fraction (x) of 1/2, and a temperature of 1500 K, we have n/V=0.0325 kg-mol/m^3.

How this is related to the concentration in the outer regions of the alumina is a question we are not equipped to answer at the present time. A fraction of the oxygen molecules dissociate on impact with the alumina surface, and so there is a flux of O atoms to this surface. The calculation of this flux also presents a challenge that we are not able to meet, particularly since at 8 atm and 1500 K the mean free path ∼20 nm and so the Knudsen layer must be accommodated. Some of this flux attaches to the surface and thence migrates into the interior; we do not know what fraction does so.

To bypass these difficulties, we assume that c_o is proportional to the concentration defined by (16). Then with the meanings of K, q and n reassigned, (15) can be replaced by

$$\frac{ds}{dt} = -K\left(\frac{x}{x_{ref}}\right)^m \left(\frac{p}{p_{ref}}\right)^q \left(\frac{T}{T_{ref}}\right)^n \exp\left[-\frac{E}{RT} + \frac{E}{RT_{ref}}\right]. \tag{18}$$

A further modification can accommodate the experimental results of Glumac, results which can be forced by replacing (18) by

$$\frac{ds}{dt} = -Ks^{0.75}\left(\frac{x}{x_{ref}}\right)^m \left(\frac{p}{p_{ref}}\right)^q \left(\frac{T}{T_{ref}}\right)^n \exp\left[-\frac{E}{RT} + \frac{E}{RT_{ref}}\right], \tag{19}$$

again with a reassignment of the meaning of K. This can be regarded as an epistemological model (of the pragmatic school), but can also be viewed in the context of Section 2. Let us write the regression law (9) in the form

$$\frac{d}{dt}\left[\frac{4}{3}\pi s^3\right] = -4\pi s^2 K \left(\frac{c_o}{c_{ref}}\right)^m \left(\frac{p}{p_{ref}}\right)^q \left(\frac{T}{T_{ref}}\right)^n \exp\left[-\frac{E}{RT} + \frac{E}{RT_{ref}}\right]. \tag{20}$$

Now suppose that the fracturing that occurs on multiple scales as the burn progresses creates a boundary surface between the aluminum and the alumina that is fractal in nature. This will have no affect on the volume, the left-side of (20), but on the right the surface area ($\sim s^2$ for a smooth surface) will then be proportional to $s^{2+\nu}$ ($0 < \nu < 1$) for some ν. The choice in (19) corresponds to $\nu = 0.75$.

4.1.1 Comparison with experimental data

When (19) is integrated (s from $d/2$ to 0, t from 0 to τ) we get

$$\tau = \frac{1}{K'}\left(\frac{d}{d_{ref}}\right)^{0.25}\left(\frac{x}{x_{ref}}\right)^{-m}\left(\frac{p}{p_{ref}}\right)^{-q}\left(\frac{T}{T_{ref}}\right)^{-n}\exp\left[\frac{E}{RT} - \frac{E}{RT_{ref}}\right],\ K' = K d_{ref}^{-0.25} 2^{-1.75} \tag{21}$$

and we compare this formula with the experimental results of [7]. We start by taking d_{ref}=80 nm, p_{ref}=32 atm, x_{ref}=0.5, T_{ref}=1460 K and with $d = d_{ref}$, $p = p_{ref}$, $T = T_{ref}$ so that $\tau = (1/K')(x/x_{ref})^{-m}$ we obtain the curve shown in Figure 2 when $K' = 0.011\mu s^{-1}$ and $m = 0.402$. Figure 2 also shows data from [7] with $\pm 15\%$ error bars, as suggested by our laboratory experience in this field. The measured temperature for which this data was obtained is 1500 K but for reasons that we describe in the next paragraph we adjusted that to 1460 K, a modest shift that does no violence to plausible error possibilities, Now with $p = p_{ref}$, $d = d_{ref}$, $x = x_{ref}$ so that

$$\tau = \frac{1}{K'}\left(\frac{T}{T_{ref}}\right)^{-n}\exp\left[\frac{E}{RT} - \frac{E}{RT_{ref}}\right],$$

we construct the lower curve of Figure 3 with the choice $n = 0.4$, $E = 56000$ J/mol-K. The upper curve, for a pressure of 8 atm, is obtained by choosing $q = 0.6$. Again, the experimental data is from [7]. It is in examining these two sets of data that we were led to the choice $T_{ref} = 1460$ K, for with a choice of 1500 K the fits are inferior unless we use different values of E for the different pressures. There can be no objection to such a strategy for there is no reason to believe that the set of true reactions which lead to an effective E at 32 atm lead to an identical effective E at 8 atm. But we are inclined to use a single E strategy if only to avoid the problem of what value of E to choose when $p = 20$ atm, for which the data of Figure 4 are relevant.

Figure 4 shows burn times vs d when p =20 atm, $T = 1550$ K, and $x = 0.2$, with experimental data from [7]. It is this data that led us to force the $d^{0.25}$ law.

4.2 Solution for general D

In general, the concentration c (equation 12) can not be approximated by c_o and the burn time must be determined by integrating equation (14) after modification to allow for the fractal boundary. Thus a choice must be made for c_o and so we start with further discussion of that issue.

It was noted earlier that for a pressure of 8 atm, a temperature of 1500 K, and a mole fraction of oxygen of 0.5, the mole concentration of O_2 is 0.0325 kg-mol/m^3. It follows that the number concentration is 0.196×10^{26} m^{-3}. Moreover, the mean molecular speed $\sim$756 m/s

corresponding to a mean speed normal to the surface of ∼481 m/s. The flux towards the surface is therefore ∼7.8 kg-mol/m^{2}s and so the flux of O atoms (albeit bound) is 15.6 kg-mol/m^{2}s, equivalent to ∼250 kg/m^{2}s. These estimates assume that the molecular motion is in thermal equilibrium, and so neglect Knudsen-layer effects, but provide a rough estimate of the maximum oxygen atom flux available for reaction with the aluminum.

This can be compared with an estimate from equation (6) (the right side) for an 80 nm particle/drop with burn time 100 μs, which yields 3.06 kg/m^{2}s, two-orders of magnitude smaller. This difference between the gas-phase flux and the required diffusive flux in the solid reflects the fact that only a small fraction of the oxygen molecules moving towards the surface end up as attached O atoms.

Attachment occurs to alumina molecules at the surface. Since the mass of an alumina molecule is 16.89×10^{-26} kg and the alumina density is 3950 kg/m^3, the molecular number density is 233.87×10^{26} m^{-3} so that the molecule spacing ∼0.35 nm. Thus the number of atom receptor sites (i.e. the number of alumina molecules) on the surface is $\sim 8.16\times10^{18}$ m^{-2}. These atoms move into the solid, one alumina molecule at a time, and to estimate the concentration near the surface we assume that on interior sheets parallel to the surface that are one alumina molecule apart (i.e. 0.35 nm apart) there are $\sim 8.16\times10^{16}$ atoms per square meter. Thus the number concentration is $\sim 2.33\times10^{26}$ m^{-3}, corresponding to $\sim$ 0.39 kg-mol/m^3. We use 0.4 for the calculations that lead to figures 5 and 6.

Consider now equation (14) with $p = p_{ref}$, $T = T_{ref}$ and the fractal factor added to K:

$$\frac{ds}{dt} = -Ks^{0.75}\left[\frac{c_o}{c_{ref}} + \left(\frac{s}{d} - \frac{2s^2}{d^2}\right)\frac{3W_{ala}\rho_{al}d^2}{4W_{al}W_oDc_{ref}}\frac{d}{dt}\left(\frac{s}{d}\right)\right]^m. \tag{22}$$

In Section 4.1.1 we solved

$$\frac{ds}{dt} = -Ks^{0.75}\left[\frac{c_o}{c_{ref}}\right]^m, \tag{23}$$

with $c_o \to x$ and $c_{ref} \to x_{ref}$, $x_{ref} = 0.5$ and chose K and m to match experimental data for different values of x. x was a surrogate for c_o - we assumed that c_o was proportional to x. We found that $K' = 0.011$ μs^{-1}, see equation (21). The same choices for K and m are sensibly used here, therefore, with $c_{ref} = 0.5$. Also, we take c_o=0.4 kg-mol/m^3.

Figure 5 shows the solution of (22) for different values of D. Note that once D exceeds 10^{-7} the trajectories are essentially indistinguishable. Figure 6 shows variations in the burn-time with particle/drop diameter. For diameters smaller than $\sim$ 300 nm the $d^{0.25}$ law is satisfied; for diameters greater than $\sim$ 1 μm a d^2 law is satisfied. The d^2 law arises by setting the right side of (22) to zero, corresponding to the vanishing of c at the front. This arises when d is large and/or D is small so that the fast-chemistry limit is achieved. It should not be confused with the d^2 law of classical fuel-drop burning, as the physics that we embrace here is quite different.

5 Conclusions

In this paper we have examined the shrinking-core model of aluminum combustion, proposed for small drops, and provided strong evidence that there is a parameter domain for which the burning rate is controlled by the reaction rate at the aluminum surface. Specifically, measured burning rate variations vs pressure variations, for example, can be correlated with pressure variations of the reaction rate. We have suggested that the alumina generated during the burning process will fracture to create cracks and voids, and that this will generate a fractal boundary which is responsible for the $d^{0.25}$ burning law observed for sufficiently small drops. For larger drops, but ones still small enough to fall within the shrinking-core framework, we have described a transition between the $d^{0.25}$ law and a d^2 law as the drop size is increased. It is important

to note, however, that this should not be confused with the classical d^2 law observed for large aluminum drops, as the physics is quite different, and the temperatures are much lower. In the discussion of the model we have examined the flux of oxygen atoms in the gas towards the drop, and noted that this flux is two orders of magnitude greater than that needed in the combustion. This suggests that the oxygen atoms at the surface of the alumina, which subsequently diffuse into the interior towards the aluminum surface, only occupy one hundredth or so of the available surface receptors, the alumina molecules. With this assumption, and assuming that the in-depth spacing of the diffusing atoms near the surface is equal to the diameter of an alumina molecule, a concentration of atoms can be estimated that yields plausible results when used in the modeling of the larger drops.

Acknowledgment

This work was supported through IllinoisRocstar LLC under grant FA9300-11-M-2004 under a Phase I SBIR program with the Air Force, program manager S. Alexander Schumaker.

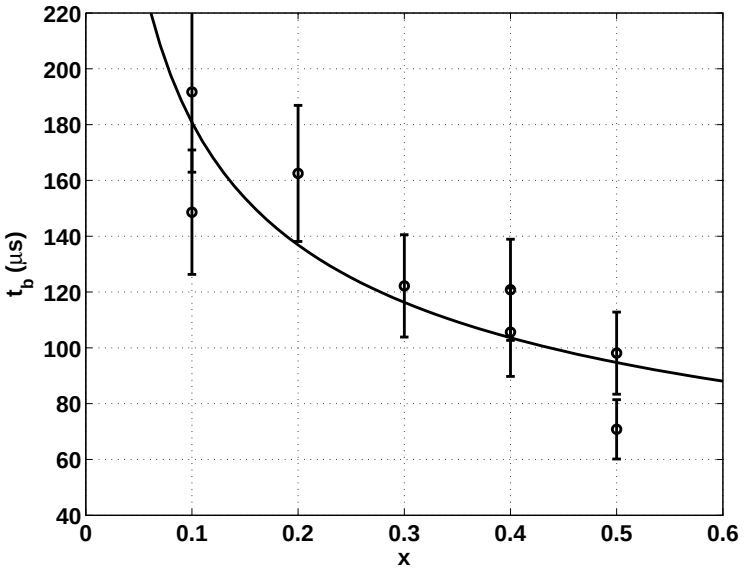

Figure 2: Burn times vs oxygen concentration, model (curve) and data (symbols) from Figure 6 of [7]. $p = p_{ref}$, $T = T_{ref}$, $d = d_{ref}$.

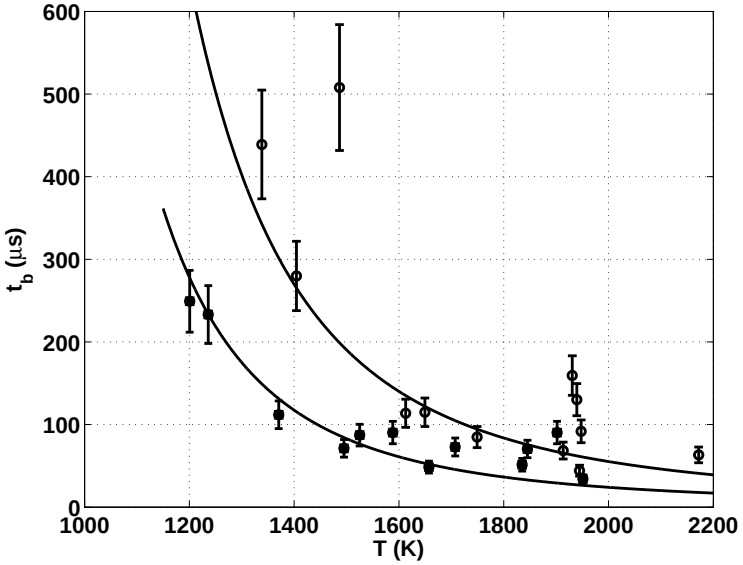

Figure 3: Burn times vs temperature at two different pressures, model (curve) and data at $p = 32$ atm (square) and $p = 8$ atm (triangle) from [7], Figure 5. $x = x_{ref}$,

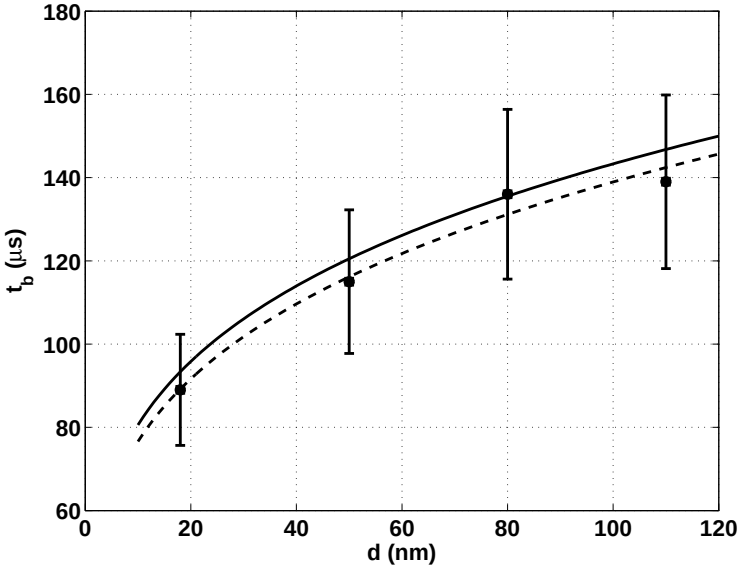

Figure 4: Burn times vs particle diameter, model (curve) and data (symbols) from [5]; $p = 20$ atm, $T = 1550$K, $x = 0.2$; the dashed curve is a Matlab fit to the experimental data, $d^{0.2586}$.

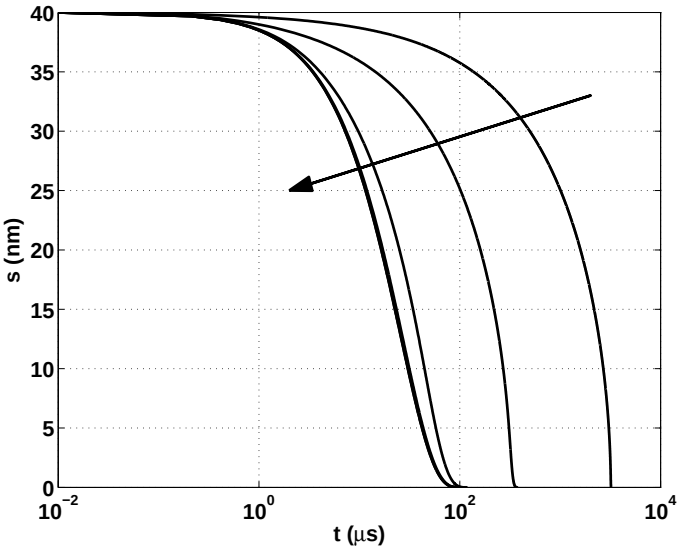

Figure 5: Variations of s with time for various D; from right to left $D = 10^{-10,-9,-8,-7,-6}$; $c_o = 0.4$, $p = p_{ref}$, $T = T_{ref}$.

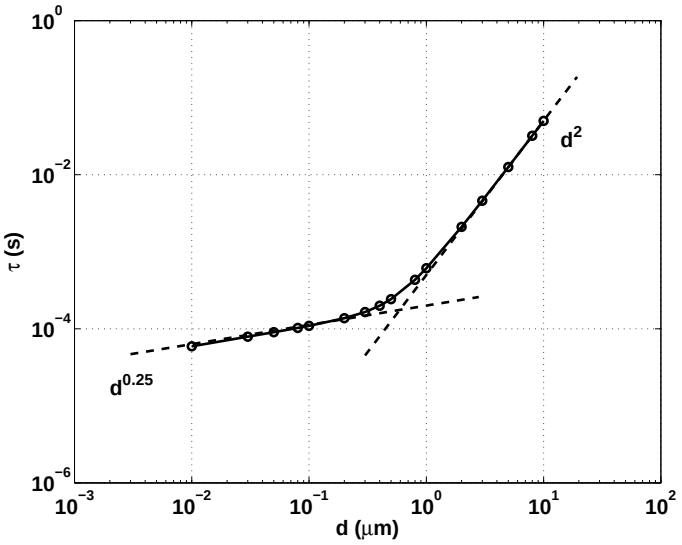

Figure 6: Variations of burn time with particle diameter d; $D = 10^{-7}\mathrm{m}^2/\mathrm{s}$, $c_o = 0.4$, $p = p_{ref}$, $T = T_{ref}$. The transition is from a $d^{0.25}$ law to a d^2 law.

References

[1] Beckstead, M.W., Newbold, B.R., and Waroquet, C. (2000). A summary of Aluminum Combustion. JANNAF 37th Combustion Subcommittee, Vol. 1, No. 701, pp. 485-504.

[2] Park, K., Lee, D., Rai, A., Mukherjee, D. and Zachariah, M.R. (2005) Size-resolved kinetic measurements of aluminum nanoparticle oxidation with single particle mass spectrometry. *J. Phys. Comm. B*, Vol. 109, pp. 7290-7299.

[3] Rai, A., Park, K., Zhou, L. and Zachariah, M.R. (2006). Understanding the mechanism of aluminum nanoparticle oxidation. *Combustion Theory and Modelling*, Vo. 10(5), pp. 843-859.

[4] Trunov, M.A., Schoenitz, M., and Dreizin, E.L. (2005). Ignition of aluminum powders under different experimental conditions. *Propellants, Explosives, Pyrotechnics*, Vol. 30(1), pp. 36-43.

[5] Glumac, N. (2011). Private communication.

[6] Aita, K., Glumac, N., Vanka, S.P. and Krier, H. Modeling the combustion of nano-sized aluminum particles. AIAA Paper 2006-1156.

[7] Bazyn, T., Krier, H. and Glumac, N. (2006). Combustion of nano-aluminum at elevated pressure and temperature behind reflected shock waves. *Combustion and Flame*, Vol. 145, pp. 703-713.